Bundled Carbon Nanotubes as Electronic Circuit and Sensing Elements

Victor T. S. Wong and Wen J. Li*
Centre for Micro and Nano Systems
The Chinese University of Hong Kong
Hong Kong SAR

**Contacting Author: wen@acae.cuhk.edu.hk*

Abstract **- Bundled multi-walled carbon nanotubes (MWNT) were successfully and repeatably manipulated by AC electrophoresis to form resistive elements between Au microelectrodes and were demonstrated to potentially serve as novel thermal and anemometrical sensor as well as simple electronic circuit elements. We have measured the temperature coefficient of resistance (TCR) of these MWNT bundles and also integrated them into constant current configuration for dynamic characterization. The I-V measurements of the resulting devices revealed that their power consumption were in μW range. Besides, the frequency response of the testing devices was generally over 100 kHz in constant current mode operation. Using the same technique, bundled MWNT was manipulated between three terminal microelectrodes to form simple potential dividing device. This device was capable of dividing the input potential into 2.7:1 ratio. Based on these experimental evidences, carbon nanotube is a promising material for fabricating ultra low power consumption devices for future sensing and electronic applications. Hence, we are currently developing fast and low cost MEMS fabrication processes to incorporate carbon nanotubes as sensing elements for various types of micro sensors.**

1. INTRODUCTION

Power consumption is one of the most important engineering considerations in designing electrical circuits and systems. Hugh amount of efforts have been placed to minimize the power consumption of electrical systems, since high power consumption implies high heat dissipation which is undesirable in many applications. A typical example is the wall shear stress measurement in aerodynamic applications [1]. Excessive heat dissipation from a hot film anemometrical sensor will disturb the minute fluidic motion, crippling its ability to sense true fluidic parameters. With our preliminary experimental findings on bundled MWNT devices, we found that the devices can be operated at μW range, which is ultra low power consumption for applications like shear stress and thermal sensing (e.g., in the order of mW range for typically MEMS polysilicon devices [2]).

Carbon nanotubes (CNT), since discovered in 1991 by Sumio Iijima [3], have been extensively studied for their electrical [4] and mechanical properties [5]. In order to build a CNT based device, technique to manipulate the CNT has to be developed. Typical manipulation technique is by atomic force microscopy [6]. However, this pick-and-place technique is time consuming, though the technique has very high positioning accuracy. Past demonstrations by K. Yamamoto et al. showed that carbon nanotube can be manipulated by AC and DC electric field [7,8]. Besides, a recent report from L. A. Nagahara et al. demonstrated the individual single-walled carbon nanotube (SWNT) manipulation using nano-electrodes by AC bias voltage [9]. By using similar technique (i.e., AC electrophoresis), we have successfully manipulated bundled carbon nanotubes to form resistive elements between Au microelectrodes for sensing and electronic circuits efficiently. This paper reports the technique to form bundled MWNT resistive element between Au electrodes and our preliminary experimental findings on the electrical characterizations such as frequency response and I-V characteristics of the bundled MWNT devices. The results indicate that the carbon nanotube is promising to be used as high performance and low power consumption devices for future electronic and sensing applications.

2. FORMATION OF CNT ELEMENTS BY AC ELECTROPHORESIS

2.1 Fabrication of Microelectrodes

Array of Au microelectrodes with different geometrical shapes (see *Figure 1*.) were fabricated on a 1.8 X 1.8 cm^2 glass substrate and silicon substrate for carbon nanotube manipulation. To start with, the substrate was first coated with Cr and Au inside e-beam evaporator and then spun with AZ5214 positive photoresist and was patterned to the desired geometries. After the patterning procedure, the Au and Cr were then etched by Au etchant ($KI : I_2 : H_2O = 4 : 1 : 80$) and Cr etchant, respectively. The photoresist was then removed by acetone or oxygen plasma. Detailed parameters for the

photolithography procedures can be found in [10].

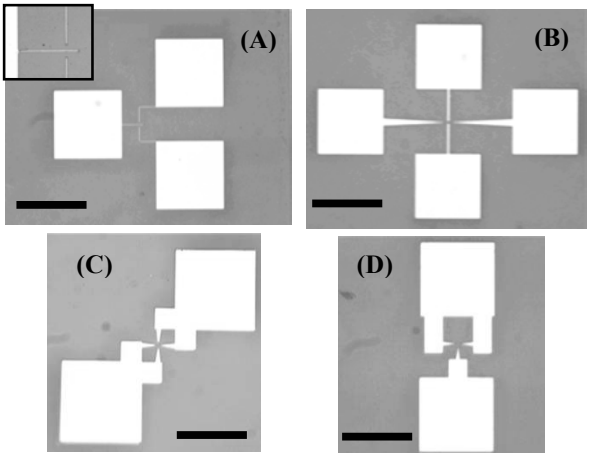

Figure 1. Different microelectrode geometries for MWNT manipulations, A) three-terminal microelectrodes to form three terminals potential dividing device (inset showing the gap (~ 5 μm) between the microelectrodes), B) four-terminal microelectrodes to form simple resistive bundled MWNT device, C) Cross microelectrodes to form parallel bundled MWNT geometry, D) T microelectrodes to form V-shape bundled MWNT geometry. (Scale Bar = 200 μm)

2.2 AC Electrophoretic Manipulation of CNT

2.2.1 Theoretical Background

AC electrophoresis (or dielectrophoresis) is a phenomenon where neutral particles undergoing mechanical motion inside a non-uniform AC electric field (see *Figure 2*). Detailed descriptions on AC electrophoresis can be found in [11]. The dielectrophoretic force imparted on the particles can be described by the following equation:

$$\vec{F}_{DEP} = \frac{1}{2}\vec{\alpha} V \nabla \left|\vec{E}\right|^2 \qquad (1)$$

where $\vec{\alpha}$ is the polarizability of the particles, which is a frequency dependent term. V is the volume of the particles and $\nabla = \vec{i}\frac{\partial}{\partial x} + \vec{j}\frac{\partial}{\partial y} + \vec{k}\frac{\partial}{\partial z}$ is the gradient operator. $\left|\vec{E}\right|$ is the magnitude of the electric field strength. Equation (1) reveals that the generated force is dependent of the gradient of electric field rather than the direction of electric field. Besides, the polarizability function also determines whether the force generated is attractive (positive dielectrophoresis) or repulsive (negative dielectrophoresis).

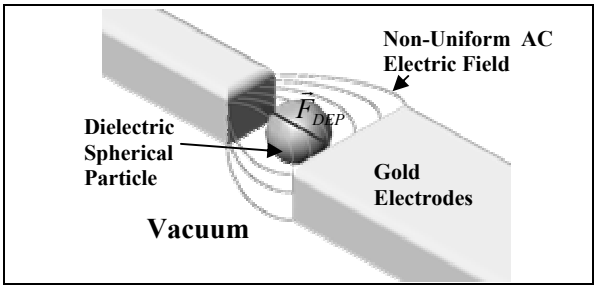

Figure 2. Under non-uniform AC electric field, dielectrophoretic force induced on the neutral particle cause the mechanical motion.

2.2.2 Experimental Details

The MWNT we used in the experiments was ordered commercially from [12] (prepared by chemical vapour deposition). The axial dimension and the diameter of the MWNT was 1 – 10 μm and 10 – 30 nm, respectively. Prior to the MWNT manipulation, 50 mg of the sample was ultrasonically dispersed in 500 mL ethanol solution and the resulting solution was diluted to 0.01 mg/mL for later usage.

After the Au microelectrodes were wire-bonded to the external circuits, approximately 10 μL of the MWNT/ethanol solution was transferred to the substrate by 6 mL gas syringe (see *Figure 3*). Then the Au microelectrodes were excited by AC voltage source (typically, 16 V peak-to-peak at 1 MHz). The ethanol was evaporated away leaving the MWNT to reside between the gap of the microelectrodes (see *Figure 4*). In *Figure 4*, room temperature resistance of 6.12 kΩ between microelectrodes was found upon two probe measurement which suggested that connection had been formed between two microelectrodes.

We experimentally found that the resistances of the MWNT bundles were sample dependent (i.e., different MWNT samples have different room temperature resistances) and the two probe room temperature resistances of the samples were typically ranging from several kΩ to several hundred kΩ. Since the conductivity of CNTs were dependent on their lattice geometries during their growth process, the conductivities of individual CNT cannot be well controlled, which results in the variation of conductivities in individual CNT. During the AC electrophoresis process to form MWNT bundles across microelectrodes, the MWNT was randomly connected between microelectrodes. Therefore, it is logically followed that different MWNT samples exhibited different conductivities.

Besides, the direction of the bundled MWNT alignments can be controlled by the microelectrode geometries. For example, in *Figure 5*, the MWNT bundles can be aligned into V-shape geometry and parallel geometry.

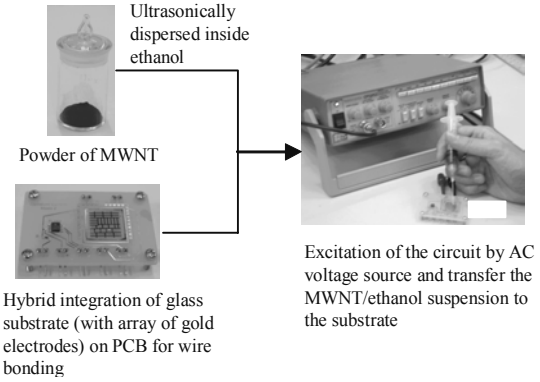

Figure 3. Experimental process flow showing the fabrication of MWNT based circuit elements.

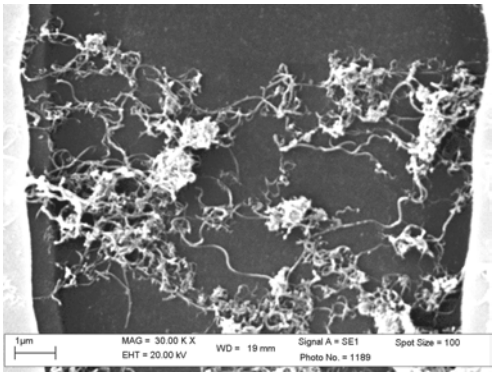

Figure 4. Scanning electron microscopic image (SEM) showing the MWNT connections between Au microelectrodes.

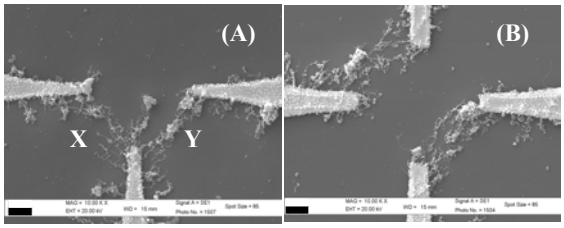

Figure 5. Special alignments of MWNT bundles. A) V-shape geometry. MWNT linkages X and Y were aligned in about 90 º . B) MWNT linkages were aligned into parallel geometry. (Scale Bar = 3 µm).

3. CNT AS THERMAL SENSING ELEMENT

3.1 Thermal Sensitivity

Bundled MWNT was served as sensing element driven in constant current mode configuration (see *Figure 6*). In order to measure the temperature-resistance relationship of the bundled MWNT device, the hybrid integrated circuit was put inside an oven (Lab-Line® L-C Oven) and the temperature of the environment was kept monitored by the Fluke type K thermocouples attached on the surface of the circuit board. The TCR was then obtained by measuring the change of resistance of the bundled MWNT with the corresponding temperature. From the experimental measurements on a typical bundled MWNT device, its resistance dropped with temperature, which is in agreement with [13] (i.e. negative TCR). Interestingly, the TCR measurements of all of our testing devices did not converge but the ranges were generally within -0.1 to -0.2 %/°C (see *Figure 7*). Considerably drifting in the room temperature resistances of the device were observed in different measurements. We suspect the variations were contributed by the mismatch in thermal coefficient of expansion between the Au electrodes and the bundled MWNT, causing some of the MWNT linkages detach from the Au electrodes, or due to contaminations such as moisture during measurements. In order to form a more robust protection for MWNT bundles, we are currently developing a process to embed MWNT bundles between parylene layers to see its effectiveness (see *Figure 8*). Nevertheless, the temperature-resistance dependency of bundled MWNT implied its thermal sensing capability. Besides, from the I-V measurement of the bulk MWNT device, the current required to induce the self heating of the device was in µA range at several volts which suggested the power consumption of the device was in µW range (see *Figure 9*).

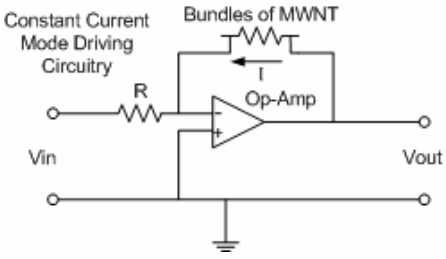

Figure 6. Schematic diagram showing the typical constant current mode configuration.

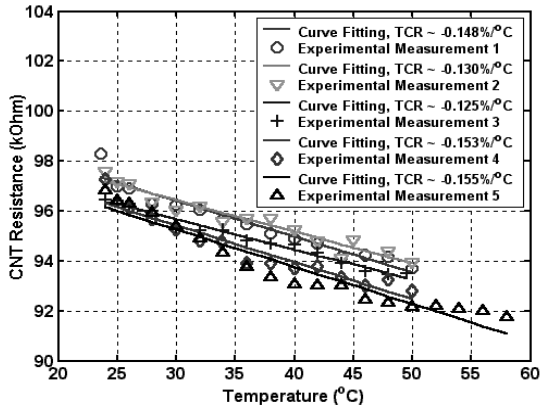

Figure 7. TCR for a typical bundled MWNT device in five different measurements.

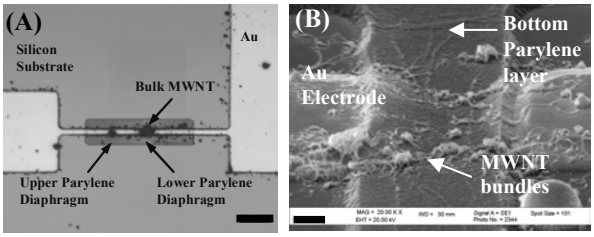

Figure 8. A) Optical microscopic image showing the prototyping parylene/MWNT/parylene device (Scale Bar = 20 μm). B) SEM image (tilted at 60 °) showing MWNT bundles resting on parylene bottom layer in MWNT/parylene configurations (without top parylene layer coating for clear visualization for MWNT bundles) (Scale Bar = 1 μm).

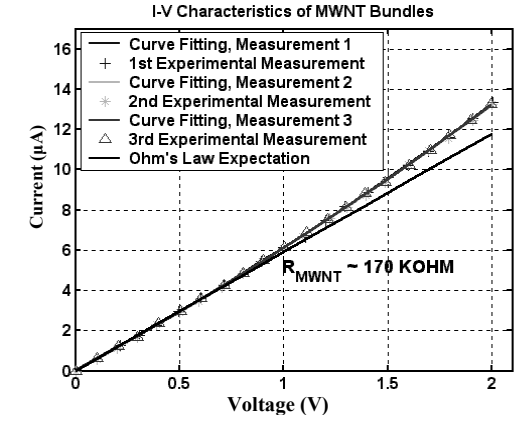

Figure 9. I-V characteristics of a typical bundled MWNT device. Three repeated measurements were performed to validate its repeatability. The straight line is the theoretical expectation using Ohm's Law and the room temperature resistance of bundled MWNT in our testing sample was about 170 kΩ .

3.2 Frequency Response

In order to pick up small variations of the sensing environment, sensors with fast frequency response are highly desired. To test the frequency response of the bundled MWNT device, input square wave of 2 V peak-to-peak at 10 kHz was fed into the negative input terminal of the circuit shown in Figure 6 and the output response was determined (see *Figure 10*.). From our experimental measurements, bundled MWNT device exhibited very fast frequency response. Using the approximation between the time constant and cutoff frequency [2],

$$f_c = 1/1.5t_c \qquad (1)$$

where f_c is the cutoff frequency, t_c is the time constant of the response, and therefore the estimated cutoff frequency of the device was about 177 kHz (see *Figure 10*). As a comparison, typical frequency response of MEMS poly-silicon sensors in constant current mode configuration without frequency compensation is around several hundred Hz to several kHz [2, 14].

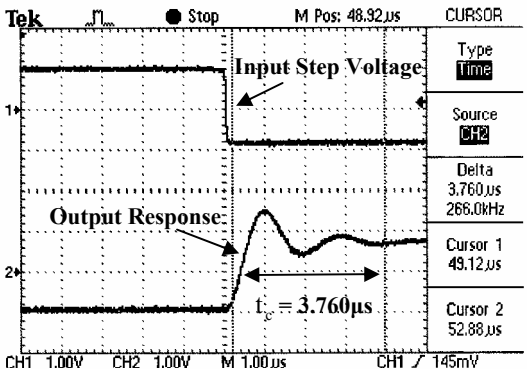

Figure 10. Frequency response of MWNT bundles in constant current mode configuration.

3.3 Bundled CNT as Sensing Element for Anemometry Sensing

A proof-of-concept experiment was performed to validate the fluid sensing ability of bundled MWNT device in μW operating power. The CNT sensor was placed perpendicular to a flow source with constant outlet velocity. The distance between the source and the sensor was then varied to induce different impinging velocities on the device (similar to Hiemenz flow) (see *Figure 11*). Although the flow environment was not well-controlled, results do clearly indicate the response of the CNT sensor to different impinging velocities (see *Figure 12*). Wind

tunnel testing on the sensors will be performed in the later stage to determine their sensitivities.

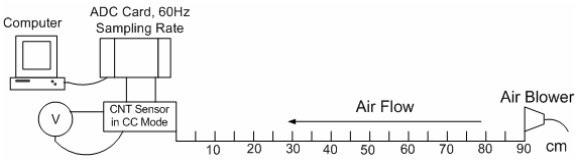

Figure 11. Schematic diagram showing the experimental setup for simple air blowing testing. The CNT sensor was placed in normal direction to the air flow.

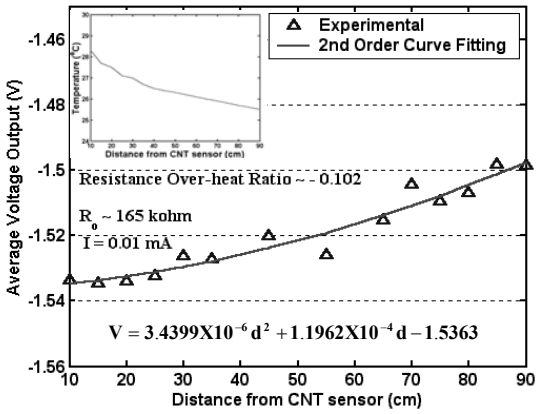

Figure 12. Output voltage variations with the air flow at different locations between the sensor and the air blower. Inset showing the temperature of the air flow at different locations and the range was generally within 2 ^{o}C . The operating power of the bundled MWNT sensor was about 15 μm .

4. CNT AS POTENTIAL DIVIDING DEVICE

Using the technique reported in Section 2, bundled MWNT were manipulated by a three terminals Au microelectrodes (see *Figure 1*A) to form simple potential dividing circuit (see *Figure 13*.). Two probe room temperature resistivity measurements for the terminals 1-2, 1-3 and 3-2 were about 1141 kΩ , 307 kΩ and 833 kΩ respectively.

We have calculated the expected voltage output of the device using the potential dividing formula of a resistive circuit,

$$V_{13} = \frac{R_{13}}{R_{12}} \cdot V_{12} \quad , \quad V_{32} = \frac{R_{32}}{R_{12}} \cdot V_{12} \qquad (2)$$

where R_{12}, R_{13} and R_{32} are the resistance across the terminal 1-2 ,terminal 1-3 and terminal 3-2 respectively. V_{12} is the voltage applied across terminal 1-2. The MWNT linkages incorporated with the three terminals microelectrodes can be used as a potential dividing circuit. The device was capable to switch the input potential into a ratio about 2.7:1 (see *Figure 14*). The I-V measurements on terminal 1-3 and terminal 3-2 revealed the power consumption of the bulk MWNT device was in μW range (see *Figure 15*).

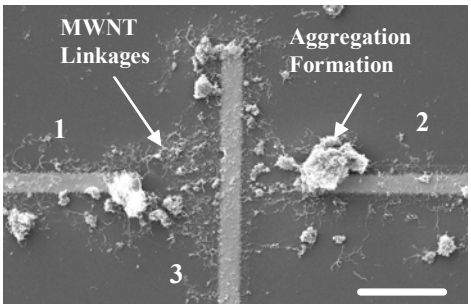

Figure 13. SEM image showing the formation of MWNT linkages with three terminals microelectrodes. Aggregation was observed and this was due to the instability of MWNT in ethanol medium. Terminals 1, 2 and 3 were indicated in the figure. (Scale Bar = 6 μm)

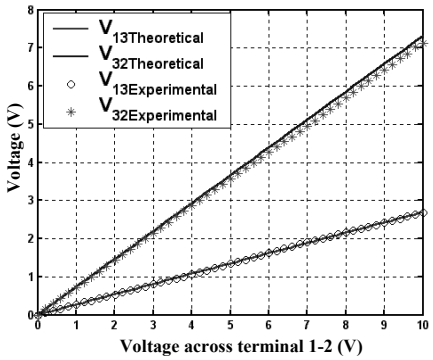

Figure 14. Comparison between the theoretical calculations and experimental results on the potential switching capability of a MWNT potential dividing circuit.

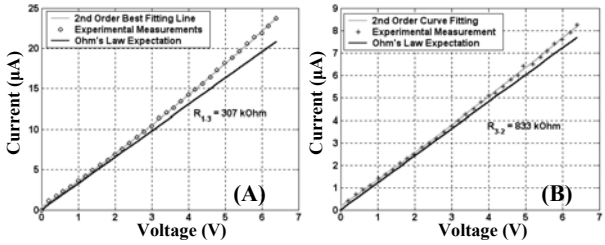

Figure 15. I-V characteristics for terminals A) 1-3 and B) 3-2. Due to the electrical conductivity dependency on different combinations of MWNT bundles, the non-linearity begun at different applied voltages in terminal 1-3 and 3-2 respectively.

5. CONCLUSION

A technique to form bundled MWNT resistive elements between Au electrodes was presented. The TCR measurements and the frequency response measurement of the bundled MWNT based device showed that bundled MWNT can be served as sensing element for high performance thermal sensing applications. Besides, the operating power of the resulting devices is in μW range which is ultra low power consumption for applications like shear stress sensing system. Apart from this, a bundled MWNT based potential dividing circuit was built with potential switching capability of 2.7:1 ratio and power consumption in μW range. From our demonstrations, bulk MWNT can be used for ultra low power consumption sensing and electrical circuit applications.

6. ACKNOWLEDGEMENTS

The authors would like to thank the Chinese University of Hong Kong (CUHK) for providing funding for this project. Besides, the authors would like to sincerely thank Dr. W.Y. Cheung of Department of Electronic Engineering of CUHK, Ms. Catherine Yeung of Department of Physics of CUHK, Mr. H.Y. Chan, Ms. W.L. Zhou, and Mr. Johnny M.H. Lee of Centre for Micro and Nano Systems of CUHK for their help and discussion for the project.

7. REFERENCES

[1] J.B. Huang, C. Liu, F. Jiang, S. Tung, Y.C. Tai, C.M. Ho, "Fluidic Shear Stress Measurement Using Surface-Micromachined Sensors", Proceedings of IEEE Region 10 International Conference on Microelectronics and VLSI, (TENCON '95), pp. 16 – 19 (1995).

[2] C. Liu, J.B. Huang, Z. Zhu, F. Jiang, S. Tung, Y.C. Tai, C.M. Ho, "A Micromachined Flow Shear-Stress Sensor based on Thermal Transfer Principle", Journal of Microelectromechanical Systems, Vol. 8, No. 1, pp. 90 – 99 (1999).

[3] S. Iijima, "Helical Microtubules of Graphitic Carbon", Nature, Vol. 354, pp. 56 – 58 (1991).

[4] S. Frank, P. Poncharal, Z.L. Wang, W.A. de Heer, "Carbon Nanotube Quantum Resistors", Science, Vol. 280, pp. 1744 – 1746 (1998).

[5] E.W. Wong, P.E. Sheehan, C.M. Lieber, "Nanobeam Mechanics: Elasticity, Strength, and Toughness of Nanorods and Nanotubes", Science, Vol. 277, pp.1971 – 1975 (1997).

[6] T. Shiokawa, K. Tsukagoshi, K. Ishibashi, Y. Aoyagi, "Nanostructure Construction in Single-walled Carbon Nanotubes by AFM Manipulation", Proceedings of Microprocesses and Nanotechnology Conference 2001, pp. 164 – 165 (2001).

[7] K. Yamamoto, S. Akita, Y. Nakayama, "Orientation of Carbon Nanotubes Using Electrophoresis", Japanese Journal of Applied Physics, Vol.35, L917-L918 (1996).

[8] K. Yamamoto, S. Akita, Y. Nakayama, "Orientation and Purification of Carbon Nanotubes Using AC Electrophoresis", Journal of Physics D: Applied Physics, Vol. 31, L34-L36 (1998).

[9] L.A. Nagahara, I. Amlani, J. Lewenstein and R.K. Tsui, "Directed Placement of Suspended Carbon Nanotubes for Nanometers-scale Assembly", Applied Physics Letters, Vol. 80, No. 20, pp. 3826 – 3828 (2002).

[10] V.T.S. Wong and W.J. Li, "Dependence of AC Electrophoresis Carbon Nanotube Manipulation on Microelectrode Geometry", International Journal of Non-linear Sciences and Numerical Simulation, Vol. 3, Nos. 3 – 4, pp. 769 -774 (2002).

[11] H.A. Pohl, "Dielectrophoresis: The Behaviour of Neutral Matter in Nonuniform Electric Fields", Cambridge University Press (1978).

[12] Sun Nanotech Co Ltd, Beijing, P.R. China.

[13] T.W. Ebbesen, H.J. Lezec, H. Hiura, J.W. Bennett, H.F. Ghaemi, T. Thio, "Electrical Conductivity of Individual Carbon Nanotubes", Nature, Vol. 382, pp. 54 – 56 (1996).

[14] J.B. Huang, F.K. Jiang, Y.C. Tai, C.M. Ho, "MEMS-based Thermal Shear-stress Sensor with Self-frequency Compensation", Measurement Science and Technology, Vol. 10, No. 8, pp. 687 – 696 (1999).